Bootstrap current generation by symmetrically injected lower-hybrid waves in a tokamak plasma

J. P. Squire,* M. Porkolab, J. A. Colborn,† and J. Villaseñor
Plasma Fusion Center, Research Laboratory of Electronics and Department of Physics, Massachusetts Institute of Technology, Cambridge, Massachusetts 02139
(Received 19 January 1994)

High poloidal beta ($\epsilon\beta_p \sim 1$) plasma equilibria produced by injection of lower-hybrid waves with symmetric spectra ($\Delta\phi=\pi$ phasing of waveguides) show evidence of substantial non-Ohmic current generation (zero loop voltage). X-ray data indicate that, while up to 30% of the current may be carried by a highly anisotropic electron tail ($\varepsilon > 30$ keV), the bootstrap current generated by an enhanced population of intermediate energy electrons ($\varepsilon \simeq 10$ keV) could account for the remaining 70% of the current.

PACS number(s): 52.35.Hr, 52.50.Gj, 52.55.Pi

The achievement of steady-state toroidal plasma operation by means of efficient non-inductively driven toroidal plasma current is one of the great challenges of current tokamak research. To date none of the proposed, or experimentally tested, noninductive current driven techniques is efficient enough to provide the necessary plasma current to ensure acceptable energy confinement in reactor scale devices [1]. However, it has been predicted nearly two decades ago that in toroidal plasma devices the so-called "bootstrap" current may contribute significantly to the total plasma current [2]. The bootstrap effect is caused by collisional untrapping of magnetically trapped particles with banana orbits in the presence of density and temperature gradients. Theory predicts that the fraction of current driven by bootstrap effects increases with the poloidal beta β_p ($\beta_p = 2\mu_0\langle p\rangle / B_p^2$, where $B_p = \mu_0 I_p / 2\pi a$ is the poloidal magnetic field in mks units and $\langle p\rangle$ is the average plasma pressure) according to the approximate relationship

$$I_{\rm bs}/I_{\rm tot} = \epsilon^{1/2}\beta_p C_{\rm bs}(\alpha_p,\alpha_T,\alpha_J,Z_i)\ , \tag{1}$$

where $\epsilon = a/R_0$ is the inverse aspect ratio of a tokamak (a is the minor radius and R_0 is the major radius) and $C_{\rm bs}$ is a value on the order of unity that depends on details of the pressure (α_P), temperature (α_T), and current (α_J) profiles along with the ion charge (Z_i). Recently, Weening and Boozer have shown that in principle, 100% bootstrap current operation may be feasible [3]. Several experiments reported on the Tokamak Fusion Test Reactor (TFTR) [4], JT-60 [5], and Joint European Torus (JET) [6] tokamaks have observed evidence of substantial bootstrap current generation (up to 80% of the total current in JT-60). Most of these experiments have relied on heating the plasma by high power neutral beam injection, although recently JET has reported 70% bootstrap current generated by ion-cyclotron-range-of-frequencies (ICRF) heating [6]. Also, pressure driven currents have been observed in a toroidal device at Princeton University (CDX-U) with electron-cyclotron-range-of-frequencies (ECRF) heating and the experimenters hypothesize that bootstrap currents maintain the discharge [7]. Presently under design by the U.S. magnetic fusion research community is the Tokamak Physics Experiment (TPX) with the ultimate goal of testing high bootstrap current operation under steady state conditions [8]. In this device electron heating and current profile control will be achieved by a combination of fast (ICRF) and lower-hybrid wave injection, while ion heating and additional current drive will be affected by neutral injection.

A novel technique for producing high β_p equilibria was pioneered in the Versator II tokamak at MIT by using the pressure supplied by a lower-hybrid driven energetic electron tail [9]. It has been demonstrated that with current drive phasing ($\Delta\phi=\pi/2$) of adjacent elements of a waveguide array launcher (or "grill") substantial poloidal beta can be achieved at low plasma currents. Nevertheless, these energetic electrons are highly anisotropic with mean energy $\langle\varepsilon_\parallel\rangle \gg \langle\varepsilon_\perp\rangle$, and therefore are not trapped. Consequently, in Ref. [9] significant bootstrap current generation was not observed. In the present work the grill is phased at $\Delta\phi=\pi$ between adjacent elements, and an intermediate energy tail is generated in Versator II with $\langle\varepsilon_\perp\rangle \sim \langle\varepsilon_\parallel\rangle \sim 10$ keV so that significant bootstrap current generation may be expected. In a reactor, bulk electrons with comparable energies, albeit at significantly higher densities than here, would be expected to generate bootstrap currents at the multi-MA level.

Versator II is a modest sized tokamak with a circular cross section, major radius $R_0 = 0.40$ m, limiter radius $a_L = 0.13$ m, and inverse aspect ratio $\epsilon = a_L/R_0 = 0.32$. The plasma is sustained by rf injection of lower-hybrid waves with a source frequency of 2.45 GHz. The rf coupler is a four-waveguide grill with a guide width of 1 cm, a guide septum thickness of 0.15 cm, and a height of 8.64 cm. For the present experiments the relative waveguide phasing was set at either $\Delta\phi=\pi/2$ (current drive) or $\Delta\phi=\pi$ (heating). For $\Delta\phi=\pi/2$, 70% of the rf power is launched preferentially in the forward direction (the electron drift direction) with a spectrum in the range

*Present address: General Atomics, San Diego, CA 92186.
†Present address: Science Applications International Corporation, San Diego, CA 92121.

$1 < N_{\parallel} (= ck_{\parallel}/\omega) < 5$, and 30% of the power is coupled in the reverse direction (opposite the electron drift direction), with $-10 < N_{\parallel} < -2$. For $\Delta\phi = \pi$, the power is launched symmetrically with a spectrum in the range $3 < |N_{\parallel}| < 7$. These waves are resonant with lower energy electrons and no net momentum is injected with the waves. Figure 1 shows a comparison of the plasma time evolution for lower-hybrid current drive ($\Delta\phi = \pi/2$) as compared to heating ($\Delta\phi = \pi$) for high $\epsilon\beta_p$ (~ 1) plasma equilibria. The only change between the two discharges is the relative phasing of the waveguides. After inductive plasma initiation, the primary transformer Ohmic heating (OH) circuit is opened, and the plasma current is allowed to decay for $t \sim 8$ ms, and subsequently 60 kW of rf power is injected. The plasma current continues to decay for approximately 10 ms longer because of a continued decrease of the applied equilibrium field and concomitant loss of energetic electrons to the plasma limiter. This is indicated in Fig. 1 by the increased hard x-ray emission from the limiter. Approximately 10 ms after the applied equilibrium field becomes constant the plasma current reaches a steady-state value at $I_p \approx 5$ kA. The plasma current is maintained in this state with zero measured loop voltage for more than five plasma skin times (for bulk plasma particles), based on calculated values and on the L/R decay rate of the Ohmic phase. The value of $\Lambda = \beta_p + l_i/2$ (where l_i is the normalized internal inductance per unit length) is calculated from measured values of the plasma current and the applied vertical magnetic field [10]. During the steady-state phase $\Lambda = 4.0 \pm 0.4$ and this implies that $\epsilon\beta_p \sim 1$. When the same experiment is carried out at lower $\epsilon\beta_p$ ($\sim \frac{1}{2}$), corresponding to higher plasma current $I_p \approx 14$ kA, steady-state plasma equilibria are also obtained with the current drive phasing. However, at $\epsilon\beta_p \simeq 0.5$ the heating phasing requires a finite applied loop voltage ($V_{\text{loop}} \simeq 0.2$ V) to maintain the plasma current.

The rf-created high energy electron distribution is studied using a radial and a tangential array of hard x-ray (HX, 20–500 keV) spectrometers (1×3 in.^{2} NaI). Figure 2 shows schematic diagrams of each array. The radial ar-

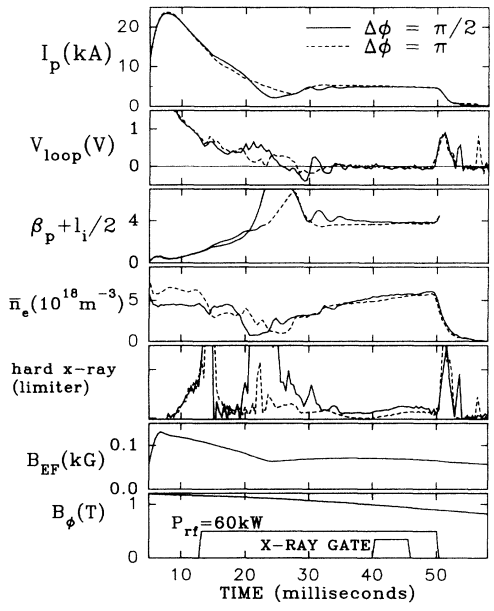

FIG. 1. A comparison of typical time evolutions of plasma current (I_p), loop voltage (V_{loop}), $\Lambda (= \beta_p + l_i/2)$, chord averaged electron density ($\bar{n}_e$), limiter hard x-ray emission, equilibrium field (B_{EF}), toroidal field (B_ϕ), and injected rf power (P_{rf}) for lower-hybrid current drive ($\Delta\phi = \pi/2$, solid lines) and heating ($\Delta\phi = \pi$, dashed lines) with high $\epsilon\beta_p (\sim 1)$. The gate pulse for the x-ray data collection is also shown. The Ohmic heating circuit is opened at $t = 7$ ms.

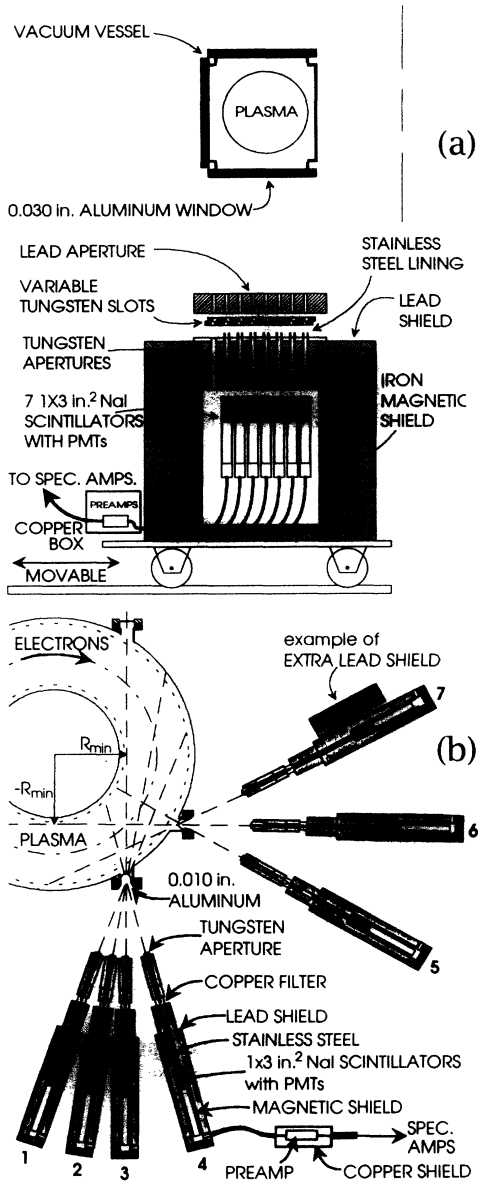

FIG. 2. (a) A side view of the NaI hard x-ray radial array used for measuring the profiles of the energetic electrons. (b) A top view of the NaI hard x-ray tangential array used for measuring the emission at a full range of angles to the toroidal magnetic field.

ray consists of seven vertically viewing detectors that can be moved between plasma shots. The tangential array uses the same detectors, which are subsequently reconfigured to view the plasma from the side of the tokamak on the midplane at seven fixed angles at a full range to the toroidal magnetic field. The configuration of this system is unique in that it has seven viewing chords ranging over all angles to the toroidal field. Consequently, no scan of a single viewing chord from shot to shot is required and there is no need to reverse the plasma current to acquire reversed angles [11]. In addition, a single soft x-ray (2–30 keV) spectrometer (SiLi) is used for viewing the plasma emission from the side of the tokamak and it can be tilted to view the entire plasma cross section [12]. Spectra are collected only during the time phase of zero loop voltage, as shown in Fig. 1 by the x-ray gate.

A verification that the equilibria are characterized by high β_p is the outward radial shift of the magnetic axis (Shafranov shift). The shift of the centroid of the density and x-ray profiles as compared to the limiter center are measured as $\Delta R/a = 0.32 \pm 0.08$. When this is taken as the Shafranov shift, theory indicates that $\beta_p = 2.9 \pm 1.0$ [10]. This along with the 4.0 ± 0.4 calculated value for Λ determines $l_i/2 \approx 1$. In order to obtain an independent measurement of l_i, we take advantage of the relationship of the x-ray profile to the current profile in a plasma equilibrium fully driven by the rf-produced electron tail. If the average parallel electron velocity $\langle v_{\parallel \text{tail}} \rangle$ and the effective ion charge Z_{eff} are approximately independent of the radius, then the current density and x-ray emission have the relationship

$$J(\rho) \propto \Gamma_{\text{HX}}(\rho)/[Z_{\text{eff}} n_{e\text{bulk}}(\rho)] ,$$

where $n_{e\text{bulk}}$ is the bulk electron density and ρ is the radius of a flux surface. For the current drive case we assume that nearly all the plasma current is carried by the high energy electron tail. Performing a least-squares fit to the energy integrated ($E_\gamma > 50$ keV) x-ray profile with a form that assumes a Gaussian current profile $[\exp(-\rho^2/w_j^2)]$ and a parabolic density profile, we find $w_j = 0.035 \pm 0.006$ m. From this we calculate $l_i/2 = 1.2 \pm 0.2$, which is consistent with the determination from the Shafranov shift. The value of q ($= B_\phi r/B_p R$) at the magnetic axis is also determined, $q_0 = 3 \pm 1$, where at the plasma edge $q_a = 40 \pm 4$.

In contrast to the current drive case, for the heating case the high energy tail most likely is not carrying the majority of the plasma current. Figure 3 shows the difference in the tangential x-ray emission for the two cases. For the current drive case there is clearly a strong enhancement in the x-ray emission in the forward direction as compared to the reverse one. This is indicative of a highly anisotropic energetic electron distribution. The heating case has similar asymmetry in the emission as the current drive case, but the intensity of the emission is lower than the current drive case by approximately a factor of 4. The limiter hard x rays also reflect this lowering in intensity, as shown in Fig. 1. This lowering represents a substantial reduction in the population of high energy

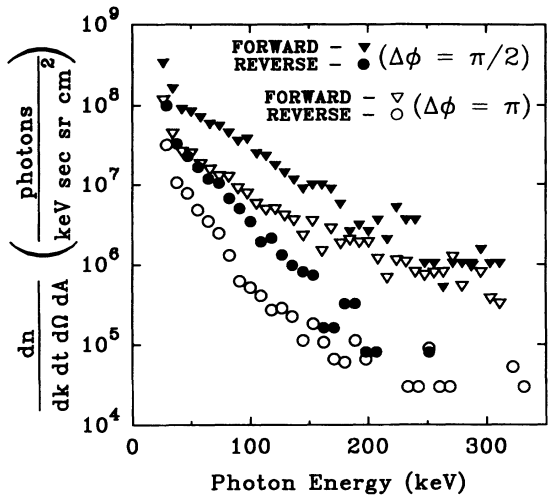

FIG. 3. A comparison of the chord integrated tangential x-ray emission for current drive ($\Delta\phi = \pi/2$, solid symbols) and heating ($\Delta\phi = \pi$, open symbols) at high $\epsilon\beta_p$. The triangles represent emission in the electron drift direction (forward) and the circles represent the opposite direction (reverse), detector numbers 1 and 7, respectively, in Fig. 2.

electrons and the current carried by these electrons.

We have carried out a quantitative analysis of the tangential x-ray emission in order to obtain information about the energetic electron velocity distribution. The analysis is performed using a computer code based on that developed by Texter *et al.* [13]. A three-temperature Maxwellian model is used in an electron-ion bremsstrahlung emission calculation. The model includes perpendicular ($T_\perp$), parallel backward ($T_{\parallel b}$), and parallel forward ($T_{\parallel f}$) temperatures relative to the toroidal magnetic field, with a high energy cutoff ($T_{\max}$) in the forward direction. A high energy halo is added to the model above the cutoff to take into account the pitch angle scattering of electrons in the forward direction. For simplicity, we assume that the velocity distribution is independent of the plasma radius, and we use the radial x-ray emission profile to determine the spatial effect on the tangential emission. We obtain a least-squares fit to the observed hard x-ray emission by iteration. The calculations are performed for all seven viewing angles of the detectors and for five separate energies ranging from 30 to 200 keV. The photon statistics of data points above 200 keV are too poor to include in the modeling procedure. The higher energy electrons, however, contribute to the lower energy emission, so the distribution model at least partially accounts for them. Furthermore, the low level of emission at the higher energies places an upper bound on the population of these electrons, which is small compared to the 30 to 200 keV tail and contributes very little to the total current carried by the tail ($< 10\%$). Figure 4 shows the best fit to observed emission for both high β_p cases.

The results for the current drive case at $\epsilon\beta_p \simeq 1$ are as follows: $T_\perp = 60 \pm 15$ keV, $T_{\parallel b} = 55 \pm 14$ keV, $T_{\parallel f} > 400$ keV, and $T_{\max} = 150 \pm 35$ keV. This gives $\langle v_{\parallel \text{tail}} \rangle / c$

$=0.23\pm0.02$, and assuming that the electron tail carries all the plasma current, we find a central tail density of $n_{\text{tail}}(0)/n_{e\text{bulk}}(0)=(1.3\pm0.3)\times10^{-2}$ and $Z_{\text{eff}}=4.6\pm0.5$. We had no independent means of determining Z_{eff}, but this value is consistent with past estimates [12]. At lower values of $\epsilon\beta_p(\sim\frac{1}{2})$ the emission profile is broader and the tail is more energetic. For the heating case, at $\epsilon\beta_p\simeq1$ the high energy tail modeling results are as follows: $T_\perp=75\pm18$ keV, $T_{\|b}=40\pm10$ keV, $T_{\|f}=195\pm48$ keV, and $T_{\max}>500$ keV, which give $\langle v_{\|\text{tail}}\rangle/c=0.21\pm0.02$. Assuming that Z_{eff} is unchanged after changing the waveguide phasings, we find that the central tail density is $n_{\text{tail}}(0)/n_{e\text{bulk}}(0)=(0.36\pm0.04)\times10^{-2}$ and that the tail only carries about 33% of the total current, namely, $I_{\text{tail}}=1.7\pm0.4$ kA. As we lower $\epsilon\beta_p(\sim\frac{1}{2})$ an externally applied loop voltage (0.2 V) is required to maintain 15 kA of plasma current, and the modeled electron tail resembles a runaway type ($T_{\max}>1$ MeV). Assuming the same Z_{eff} as the comparable current drive case, this runaway tail accounts for a majority of the plasma current.

The waves launched by the heating phasing are expected to be resonant with intermediate energy electrons with energies below 30 keV. To investigate these electrons, we construct a composite spectrum of the x-ray emission over the energy range of 2–350 keV by using the soft x-ray detector set on the midplane and the hard x-ray detector that has the corresponding view of the plasma. In order to make the geometric correction for the soft x-ray collimator consistent with the hard x-ray collimator, we assume the spectrum is continuous around 30 keV for the current drive case. For the current drive case, the electron distribution model determined from only high energy emission (>30 keV) accounts for the majority of the soft x-ray emission (<30 keV). In contrast, Fig. 5(a) shows that the calculated emission from the high energy model for the heating case accounts for less than one-half the observed soft x-ray emission. To reconcile the difference in the soft x-ray emission, an isotropic Maxwellian electron distribution with an intermediate temperature is added to the high energy model. Figure 5(a) in-

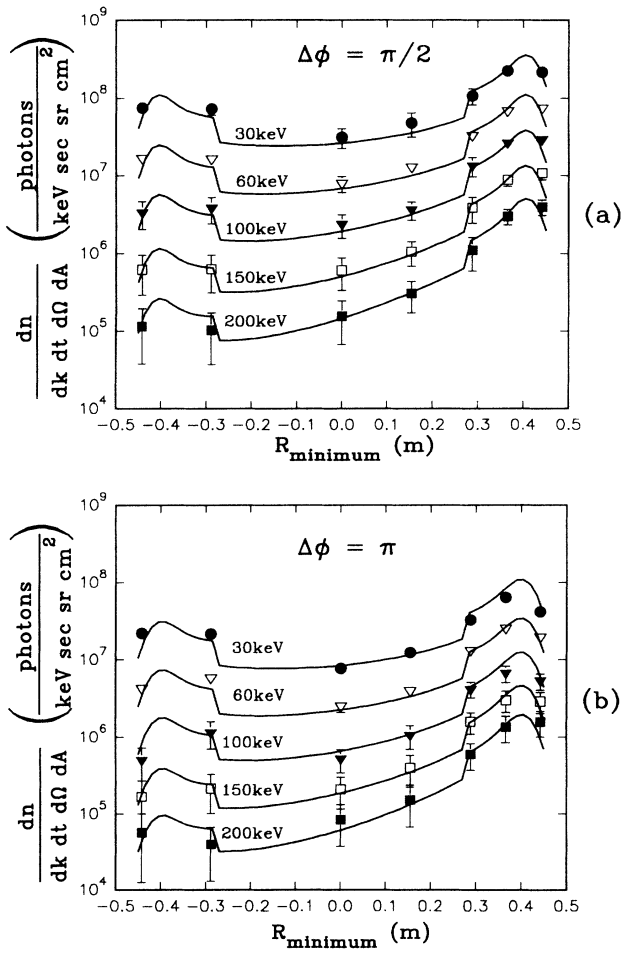

FIG. 4. The best fit of the calculated emission (solid lines) to the measured (symbols) emission plotted as a function of the minimum viewing chord radius relative to the tokamak axis (see Fig. 2). The breaks in the emission at $\pm0.28m$ correspond to the inside wall cutting off the viewing chord. (a) For $\Delta\phi=\pi/2$ phasing. (b) For $\Delta\phi=\pi$ phasing.

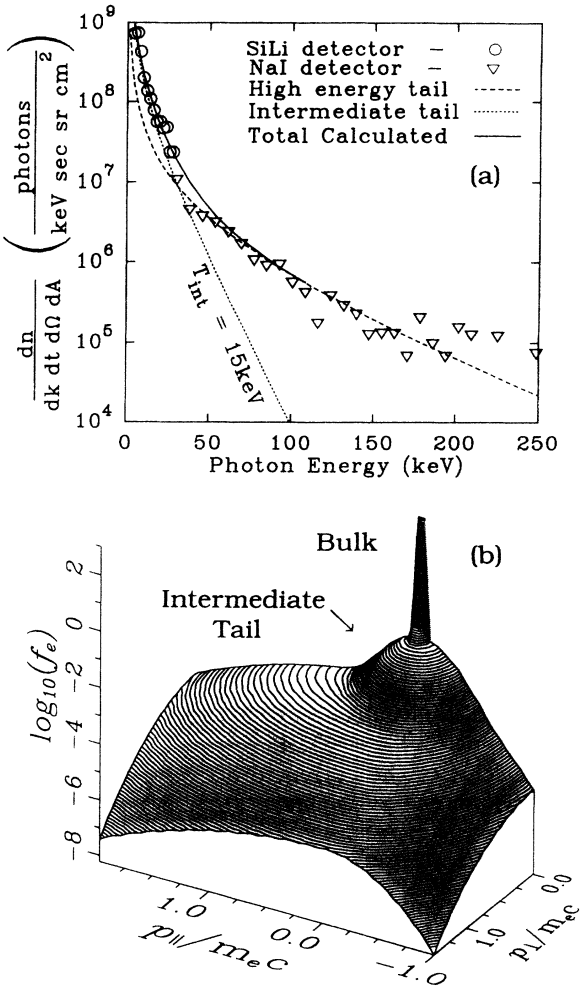

FIG. 5. (a) The measured and calculated chord integrated perpendicular x-ray emission for lower-hybrid heating ($\Delta\phi=\pi$) at high $\epsilon\beta_p(\sim1)$. (b) The total modeled normalized electron distribution function showing three components: bulk, intermediate energy tail, and high energy anisotropic tail.

cludes the best fit to the soft x-ray (SX) emission, which is $T_{\rm int}=15\pm4$ keV and $n_{\rm int}(0)/n_{e\rm bulk}(0)=(1.0\pm0.2)\times10^{-2}$. Here we use a Gaussian profile with a half-width of $w_{\rm SX}=0.07\pm0.007$ m which is determined from the soft x-ray profile. Figure 5(b) shows the total modeled electron distribution function.

The presence of an intermediate energy tail in the lower β_p heating case, although not observed because of the strong emission from the runaway electrons, is consistent with the lower resistivity of the plasma discharge and the presence of runaway electrons. A purely Ohmic discharge with the same current and density requires a loop voltage of approximately 1.5 V to arrest the current decay, as compared to 0.2 V with heating. While for the bulk electrons the applied electric field is small compared to the Dreicer field ($E/E_D \ll 1$), for the 15 keV population the electric field is large enough ($E/E_D \gtrsim 0.1$) to significantly effect the electron distribution [14]. The high energy tail in the high β_p heating case may be due to a small residual electric field in the center of the plasma, as evidenced by the asymmetric fast electron distribution. A residual electric field may remain for times longer than the resistive (bulk) L/R time because of the lower resistivity of the intermediate energy tail.

The most likely explanation for the missing current in the lower-hybrid heating case is the generation of bootstrap current. The zero measured loop voltage and the symmetrically launched wave power spectrum eliminate other possible sources of current. We can calculate the bootstrap current generated by the intermediate energy electrons using an expression originally derived by Hirshman [15]. The intermediate energy electrons, being more collisional, are nearly isotropic and therefore have a larger trapped fraction. Nevertheless, they are still in the collisionless regime for neoclassical effects, namely, $\nu_{*e}<10^{-3}$ where $\nu_{*e}=\nu_{ee}/\omega_B\epsilon^{3/2}$, with $\omega_B=v_{te}/Rq$ being the bounce frequency of electrons. In contrast, the bulk electrons ($T_{e\rm bulk}\sim100$ eV) are in the collisonal regime since $\nu_{*e}>20$. Soft x-ray spectra acquired from the outer region of the plasma indicate that the intermediate electron temperature is nearly independent of the radius, so the electron temperature $T_{\rm int}$ is taken as constant. The predicted bootstrap current may be written in the following form [16]:

$$I_{\rm bs}({\rm MA})\approx 2.5\left[\frac{R_0}{m}\right]\left[\frac{B_0}{T}\right]\left[\frac{p_{\rm int}(0)}{B_0^2/2\mu_0}\right]\times\int d\rho\, q(\rho)\frac{p_{\rm int}(\rho)}{p_{\rm int}(0)}L_{31}\left[\frac{1}{n_{\rm int}}\frac{dn_{\rm int}}{d\rho}\right], \quad (2)$$

where L_{31} is Hirshman's [15] L_{31}/j_0 and is a value on the order of $(2\epsilon)^{1/2}$, and is dependent on the ion charge and the fraction of trapped particles on a given flux surface. The intermediate energy electron density profile is determined from the soft x-ray profile and is modeled as parabolic to the power $\alpha_{\rm int}$, where $\alpha_{\rm int}=2$ best fits the data. The current profile is modeled similarly but $\alpha_J+1=q_a/q_0$. There is a large uncertainty in the value of q at the magnetic axis, while at the plasma edge $q_a=40\pm4$. Therefore the total bootstrap current is calculated for a wide range of q_0 ($=2-8$). Our estimates indicate that for this range of q_0 the bootstrap current generated by the intermediate energy electron tail is of the magnitude $I_{\rm bootstrap}\simeq4\pm1$ kA. Combined with the current from the high energy tail, this accounts, within experimental uncertainty, for the total measured plasma current of $I_p=5$ kA.

In conclusion, we find that at high values of $\epsilon\beta_p(\sim1)$ symmetric (heating phasing, namely, $\Delta\phi=\pi$) lower-hybrid wave injection generates nearly the same plasma current as asymmetric wave injection (current drive phasing, namely, $\Delta\phi=\pi/2$). By means of x-ray analysis we have determined that in the heating phasing case only one-third of the plasma current could be accounted for by the energetic electron tail. The soft x-ray emission, however, indicates an enhanced intermediate energy population of electrons. Calculations show that this tail could account for the majority ($\gtrsim70\%$) of the plasma current in the form of bootstrap current. This experiment supports the prospect of substantial bootstrap current generation in future noninductively driven tokamaks such as TPX. The fraction of the total current carried by bootstrap current and the energy of the electrons involved is very similar to proposed equilibria in TPX (although in TPX the current, power, and the number of 10 keV electrons is expected to be higher by several orders of magnitude). The experimental method presented in this paper may be used to study in detail the physics of high bootstrap current fraction equilibria using existing tokamaks at low cost.

The authors would like to acknowledge the diligent technical assistance of Edward Fitzgerald and John Fitzgerald. This work was supported by the U. S. Department of Energy under Contract No. DE-AC02-78ET-51013.

[1] N. J. Fisch, Rev. Mod. Phys. **59**, 175 (1987).
[2] R. J. Bickerton, J. W. Connor, and J. B. Taylor, Nature (London) **229**, 110 (1971).
[3] R. H. Weening and A. H. Boozer, Phys. Fluids B **4**, 159 (1992).
[4] M. C. Zarnstorff *et al.*, Phys. Rev. Lett. **60**, 1306 (1988).
[5] M. Kikuchi *et al.*, Nucl. Fusion **30**, 343 (1990).
[6] C. D. Challis *et al.*, in *Proceedings of the Europhysics Topical Conference on RF Heating and Current Drive of Fusion Devices,* edited by C. Gormezano, P. U. Lamalle, and R. R. Weynants (European Physical Society, Brussels, 1992), Vol. 16E, p. 109.
[7] C. B. Forest *et al.*, Phys. Rev. Lett. **68**, 3559 (1992).
[8] W. M. Nevins *et al.*, in *Proceedings of the 14th Interna-*

tional Conference on Plasma Physics and Controlled Nuclear Fusion Research, Wurzburg, Germany, 1992 (International Atomic Energy Agency, Vienna, 1993), Vol. 3, p. 279.

[9] S. C. Luckhardt *et al.*, Phys. Rev. Lett. **62**, 1508 (1989).

[10] J. P. Freidberg, *Ideal Magnetohydrodynamics* (Plenum, New York, 1987).

[11] J. P. Squire *et al.*, in *Proceedings of the 1992 International Conference on Plasma Physics,* edited by W. Freysinger *et al.* (European Physical Society, Innsbruck, 1992), Vol. II, p. 965.

[12] M. J. Mayberry, Ph.D. thesis, Massachusetts Institute of Technology, 1985.

[13] S. C. Texter *et al.*, Nucl. Fusion **26**, 1279 (1986).

[14] H. Dreicer, Phys. Rev. **115**, 288 (1959).

[15] S. P. Hirshman, Phys. Fluids **31**, 3150 (1988).

[16] W. M. Nevins (private communication).

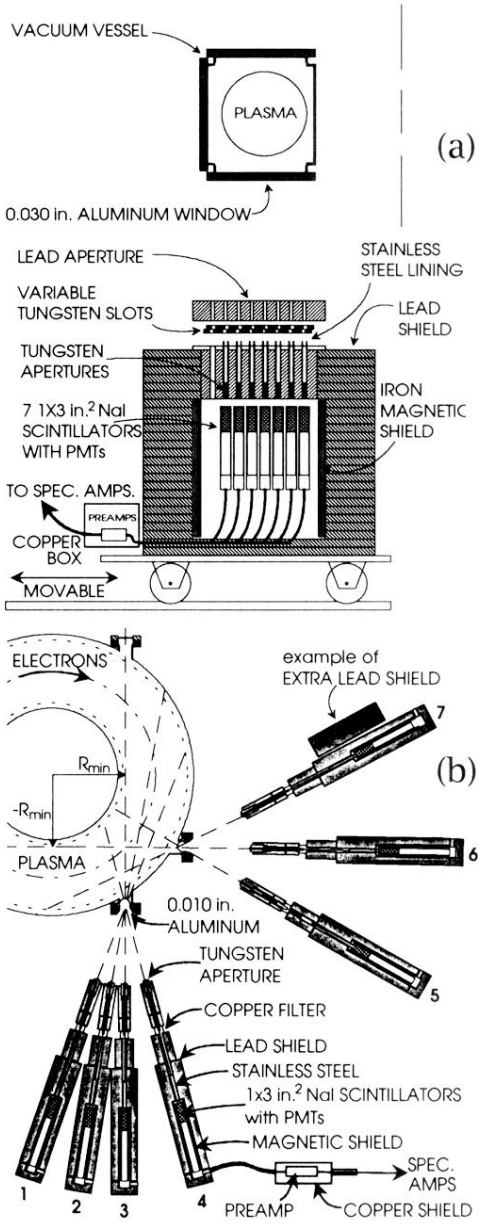

FIG. 2. (a) A side view of the NaI hard x-ray radial array used for measuring the profiles of the energetic electrons. (b) A top view of the NaI hard x-ray tangential array used for measuring the emission at a full range of angles to the toroidal magnetic field.

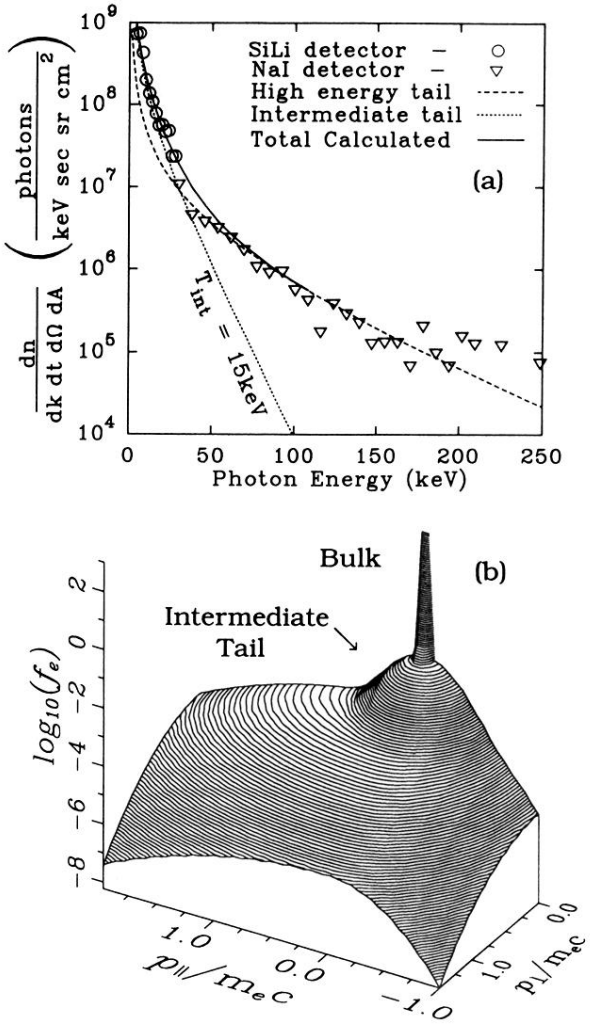

FIG. 5. (a) The measured and calculated chord integrated perpendicular x-ray emission for lower-hybrid heating ($\Delta\phi=\pi$) at high $\epsilon\beta_p(\sim 1)$. (b) The total modeled normalized electron distribution function showing three components: bulk, intermediate energy tail, and high energy anisotropic tail.